IN THE UNITED STATES PATENT AND TRADEMARK OFFICE

Applicant	:	John Harra
Title	:	APPARATUS FOR PROCESSING, STORING, AND DISPENSING SOFT SERVE FROZEN FOOD PRODUCT
Application No.	:	10/552,561
Filing Date	:	October 11, 2005
Art Unit	:	Frederick Nicolas
Examiner	:	Unknown
Attorney Docket No.	:	JH-1PCT

June 15, 2009

Commissioner for Patents
P.O. Box 1450
Alexandria, VA 22313-1450

Declaration of Robert Blinn

I currently am a design engineer for Portent Technologies, located in New York, New York. My responsibilities as a design engineer include designing machinery in 3d CAD and creating schematics for its manufacture, analyzing fluid flow and material stress in machinery via finite element analysis, and aiding in new product design.

I hold a Masters degree in Industrial Design from Pratt Institute in Brooklyn, New York and Bachelor of Mathematical Economics from Brown University in Providence, Rhode Island. In addition I have taken courses in Operations Research, Econometrics, and History at the London School of Economics in London, England.

My computer skill set includes in depth knowledge of software, including Solidworks and CF Design.

I am familiar with the content of the patent application identified above and the January 14, 2009 Office action in the application, including Curry US Patent 5,030,465 ("the Curry patent") cited in the Office Action.

Page 3 of the Office Action sets forth a rejection of claims 12-30, as being anticipated by the Curry patent:

> "Curry et al. disclose a soft serve food product manufacturing, storage and dispensing machine (col. 1 ll. 7-11), which comprises a source (21) of soft serve food product, *a closed loop circulation system* ***(as seen in Figure 2)*** adapted to receive soft serve food from the source, the closed loop circulation system *comprising an emulsification assembly (25,23,32) adapted to emulsify soft serve product in the closed loop circulation system*, a dispensing head (44) connected to the closed loop circulation system adapted to dispense soft serve food product from the closed loop circulation system ..."

Superimposing those drawings over Curry patent Figure 2 along with color coded fluid paths (see Figure A) demonstrates that Curry does not provide for "an emulsification assembly adapted to emulsify soft serve product in the closed loop circulation system." Instead, the Curry patent refers to a freeze tube assembly 32 in an open loop system also comprising a refrigerated source of liquid food substance 21 in series with a pump 30. The only closed loop system in the Curry patent is the refrigeration system which includes the refrigeration jacket of the emulsification tube 32 along with coolant from a refrigeration circuit 56 for the refrigerated source of liquid food substance 21. The refrigerant system does not connect with or include the food path.

Figure A: Curry Figure 2 with Figs. 4 and 6 superimposed (color added)

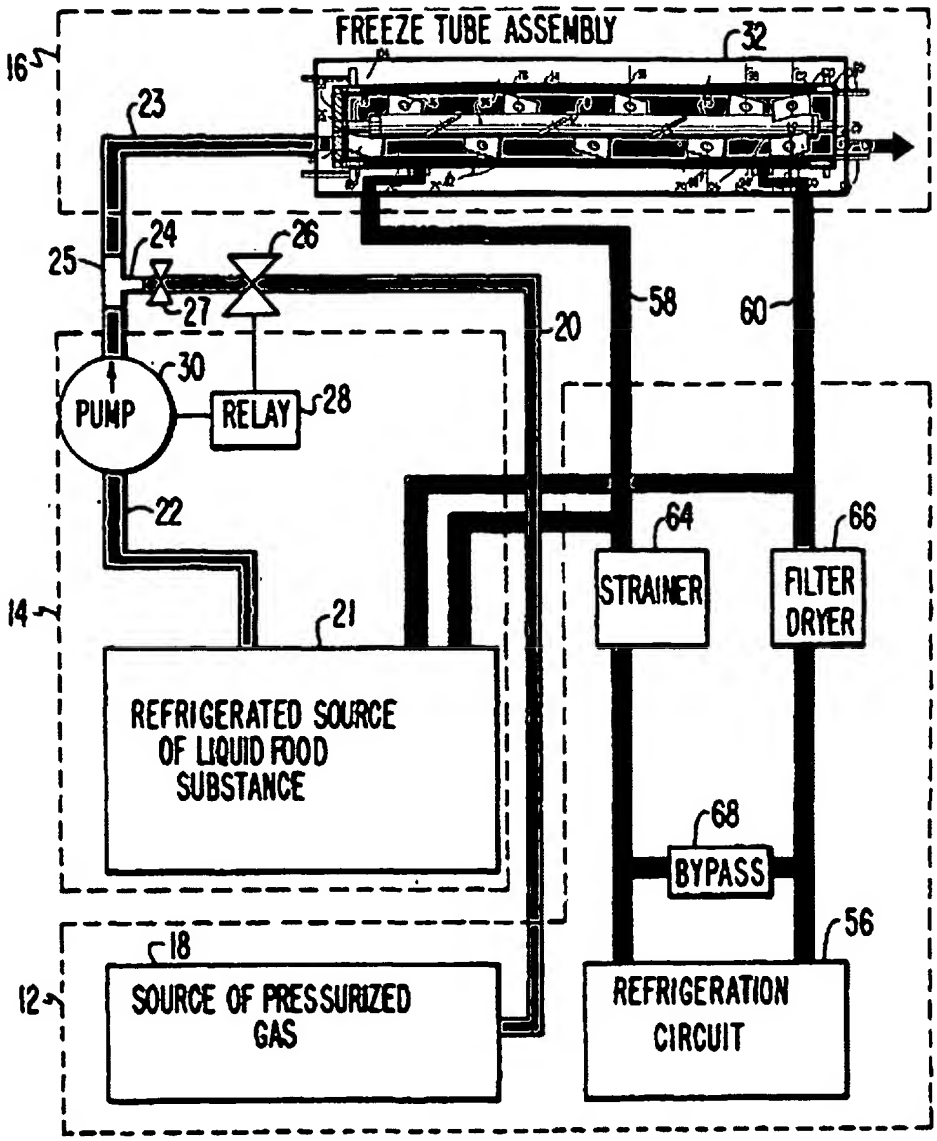

According to the Curry patent, "freeze tube assembly 32 of production unit 16 is connected via food line 22 to source of liquid food substance 21." In Figure A, this path has been colored orange. Additionally, "a pressurized source of gas 18 (preferably nitrous oxide) is stored in unit 12 and is connected via gas line 20 to food line 22." In Figure A, this path has been colored green.

Figure B: Curry Figure 4 reproduced (arrow to show direction of flow added -- Figure must be rotated 180 degrees to fit into Curry Figure 2 and consequently, Figure A)

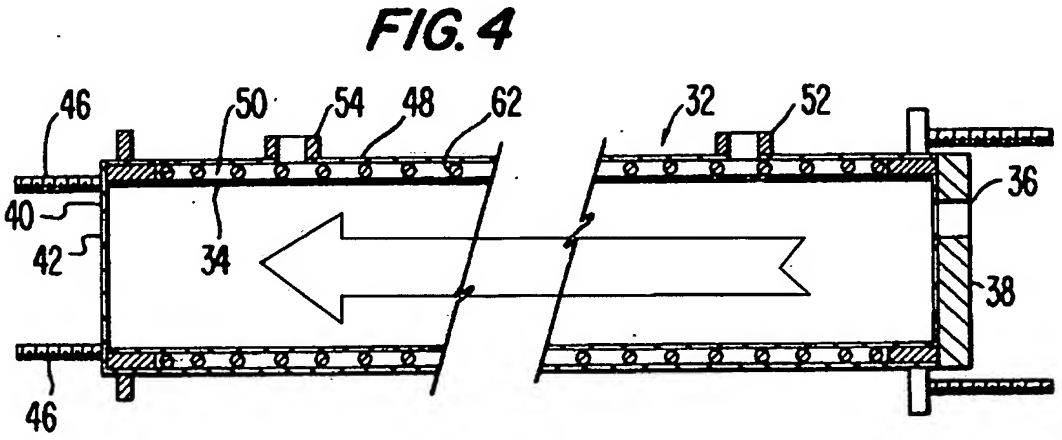

Additional detail can be found in Figure 4 of the Curry patent (shown in Figure B), as well as superimposed into the freeze tube assembly 32 in Figure A. In the Curry patent Figure 4, the "mixing portion 23 of food line 22 conducts the mixture into freeze tube assembly 32 through port 36." Since this occurs on the right side of Figure 4 and the left side of Figure A, Curry Figure 4 must be rotated 180 degrees to fit into in Figure A, where the inlet is on the left. Likewise in Figure 4, the exit is on the left: "dispensing port 42 is disposed in plate 40 for permitting frozen end product to exit freeze tube 34," while in all of Curry's other figures, the exit is on the right.

Separately, Curry states "refrigeration circuit 56 is also disposed in unit 12 and is connected via refrigeration lines 58 and 60 to freeze tube assembly 32 and insulated compartment 15." In Figure A, this path has been colored blue. Curry patent Figure 4 once again clarifies the path of fluid in the refrigeration system. In this case, "cooling means include cooling wall 48 disposed about freeze tube 34 and spaced a predetermined distance therefrom to define space 50 therebetween. Inlet port 52 and outlet port 54 are disposed in cooling wall 48 and are connected to refrigeration circuit 56 via lines 58 and 60 respectively." Consequently, Curry Figure 4 demonstrates that the paths 58 and 68 do form a circulation loop, but for refrigerant only rather than ice cream.

Further, freeze tube assembly 32 of the Curry patent cannot emulsify ice cream. Because it lacks a break bar or fins, high viscosity fluids like ice cream will be pulled around in circles in a solid cylindrical mass rather than mixed or emulsified.

Despite descriptions such as "the whipping means propelling a first portion of the mixture in a first direction from the inlet end of the tube means toward the outlet end and for simultaneously propelling a second portion of the mixture in a direction from the outlet end toward the inlet end of said tube means," the Curry patent's freeze tube assembly chamber does not provide for "a closed loop circulation," or indeed any "circulation" other than rotation about the axis. For one, the chamber defined by the

freeze tube assembly 32 is simply a container that does not include, and is not associated with, any sort of loop. To verify that the material in Curry's freeze tube assembly 32 revolves around the axis of the freeze tube rather than circulates, a computational fluid dynamics ("CFD") simulation was run with dimensions proportional to the structure shown in the Curry patent.

Project scope:

The simulation was conducted using CFdesign version 10.0 from Blue Ridge Numerics, Inc. The analysis consisted of a motion-driven flow simulation inside a fully enclosed system. The ice cream CAD model was designed using SolidWorks 2008, SP4.0.

Simulation Assumptions:

Several assumptions were made for the ice cream simulation and are listed below:

- Constant density of 1100 kg/m^3
- Non Newtonian fluid with variable viscosity based on local strain rate (See viscosity of soft serve ice cream Mix exhibit below. Source Byars)
- Stress strain curve was done using a piecewise linear mapping of 25 datapoints off of logarithmic chart from Byars' (Figure C) -- see "References"
- Completely sealed enclosure
- Smooth blade surfaces
- Clockwise blade rotation (as seen from the drive shaft end)
- 45 RPM (speed referenced in Curry patent)

Figure C: Viscosity of Soft Serve Ice Cream Mix: from Byars, with datapoints added

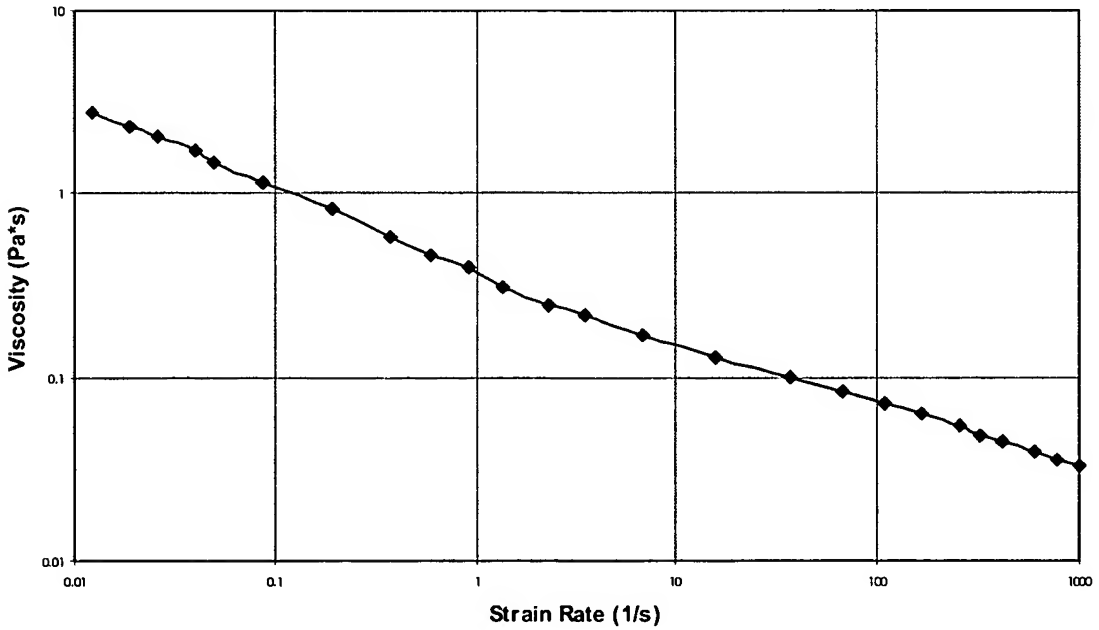

Figure D: Solidworks model superimposed over Curry Figure 6

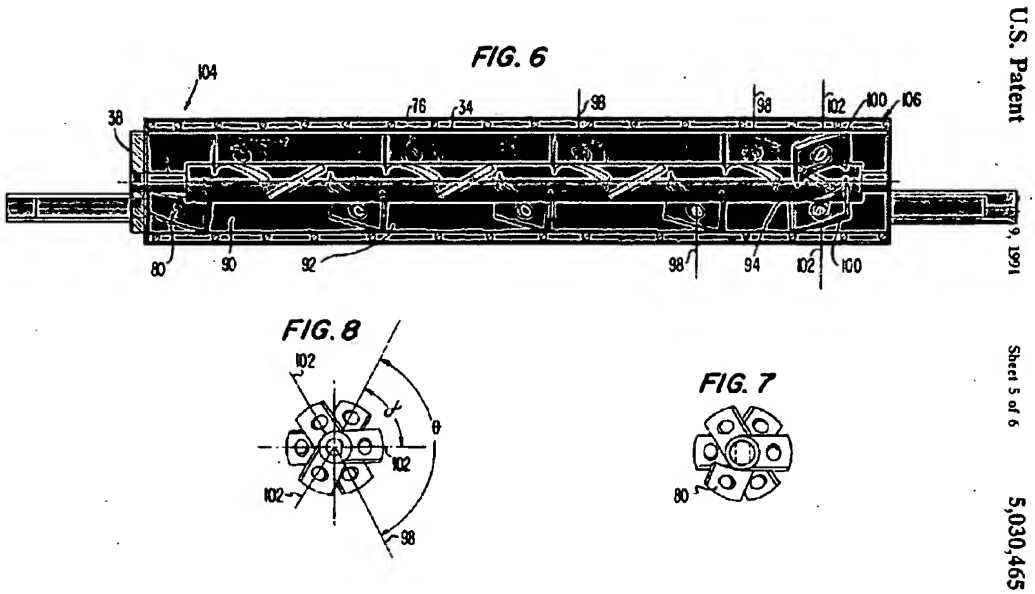

See Figure D for a comparison of the 3D model with Curry's Figures 4 and 6. Since the Curry patent was created before the popularization of 3D design, some discrepancies exist, but the 3D model was made to be mathematically consistent with the verbal description of the patent rather than accounting for possible artist errors.

Figure E: Velocity vectors at evenly spaced paddles (black background for contrast)

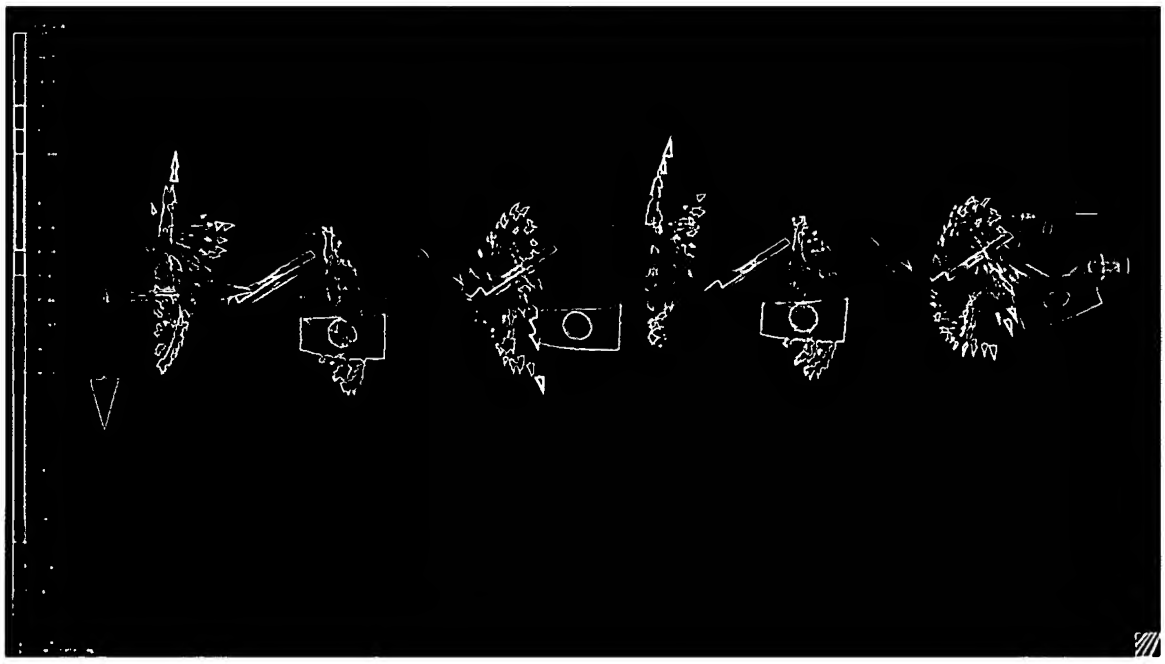

Once the model had been completed, the CFD analysis was run. Analysis showed that the holes in the paddles did not influence axial fluid movement. Viewing the apparatus in perspective with vectors representing velocity at evenly spaced cross sections shows that despite the pitch of the paddles, the fluid revolves around the center axis rather than traversing the chamber (Figure E).

Figure F: Velocity vectors showing direction of rotation and collision (black background for contrast)

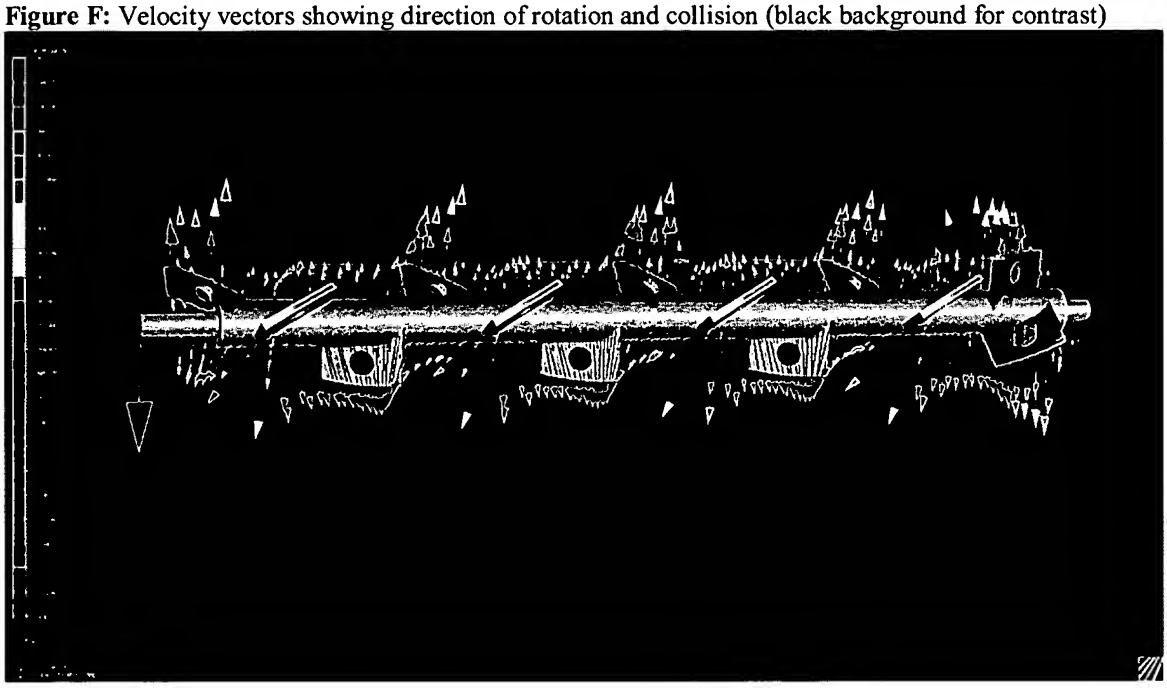

Figure F shows the rotary component of the vectors off of the XZ plane, which overwhelms their lateral motion. Statistical analysis of over 2,800 vectors originating on the XZ plane demonstrated that the average rotary component of the vectors was over 5 times as strong as the average lateral component. Additionally, any lateral motion at one location is cancelled out by adjacent vectors pointing in the other direction, while rotary motion is reinforced by other paddles rotating in the same direction. Thus any small lateral movements serve only to shuffle the mass as the paddles pass rather than providing circulation from the inlet to the outlet in any dependable manner.

Figure G: Planar view of x-axis velocity represented as color

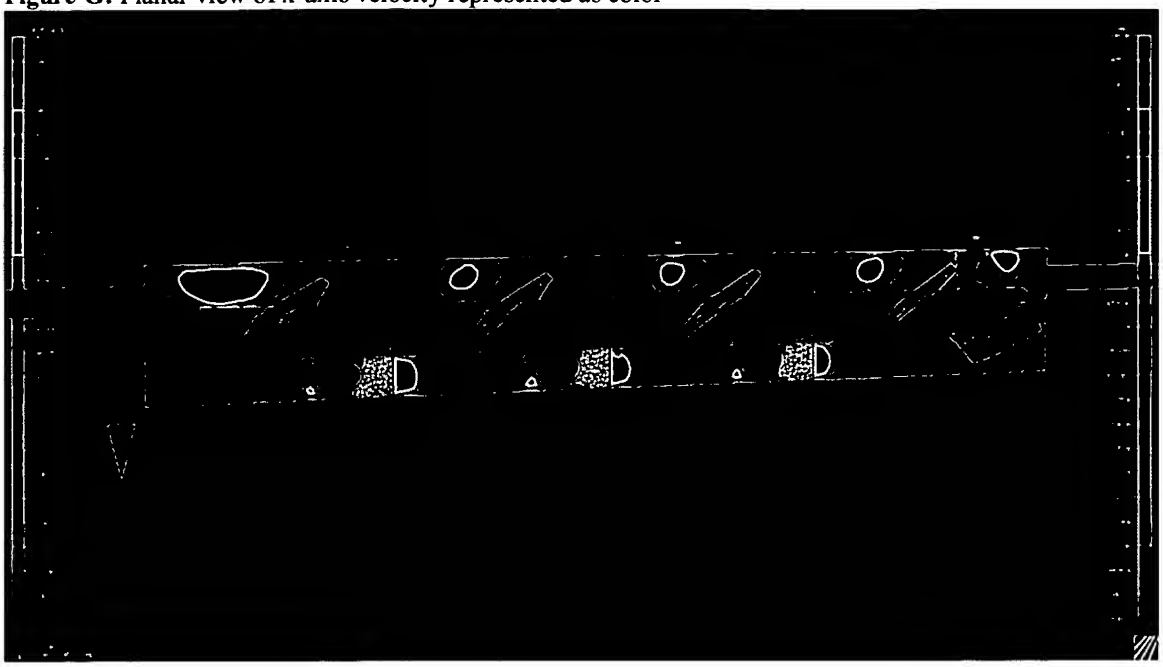

Figure G shows a cross section of the XY plane, with color representing only the X-axis (lateral) component of velocity. The black lines show the wireframe mesh used to model the shaft for CFD analysis. Green represents no lateral movement. Red and orange represents positive-X movement (distal) and Blue to Aqua represents movement in the negative-X direction (proximal). It is important to note that movement in the X axis is very small relative to overall velocity (less than 1/5th the magnitude), with the largest distal movements coming off of the trailing edge of the paddles rather than through the holes as described in the Curry patent. Further, any lateral movement is offset by opposing forces, as described below.

If circulation were to exist, a clear path could be traced where fluid at the proximal and distal ends would tend to change places over time. Instead, fluid moves away from the impellers toward areas without impellers. Since the impellers are spaced evenly and radially alternating, the fluid surges and crashes against its neighbors. This could be seen quite clearly in the alternating spots of color between aqua and orange in Figure G as well as in the collision of vectors in Figure F. As the impeller rotates, the orange and aqua spots alternate in a pulsating pattern. Clear patterns of surging back and forth emerge where fluid behaves predictably depending upon where the shaft is in its rotation. The alternation of positive and negative X movement is akin to shuffling a deck of cards where each card may randomly trade places with its neighbors. As each paddle passes by, it pushes some fluid to distal end and some to the proximal end. Curry's description indicates that the holes in the paddles push fluid toward the proximal end, but the CFD analysis does not prove this out. Looking at Figure G, the tiny aqua spots in the center of the holes as the paddles pass the plane are far smaller, and far less blue than the void left in spaces where the paddle is not.

Although the paddles are arranged in a helix, fluid does not travel along them in a helical pattern. Instead, because the fluid body is not bounded it is likely to travel from a high to a low pressure area with the nearest low pressure area tending to occur in the same paddle area. This is most clearly shown by particle trace studies, which represent the most likely paths of individual particles through the fluid body.

Figure H: Particle traces, clustered around evenly spaced blades

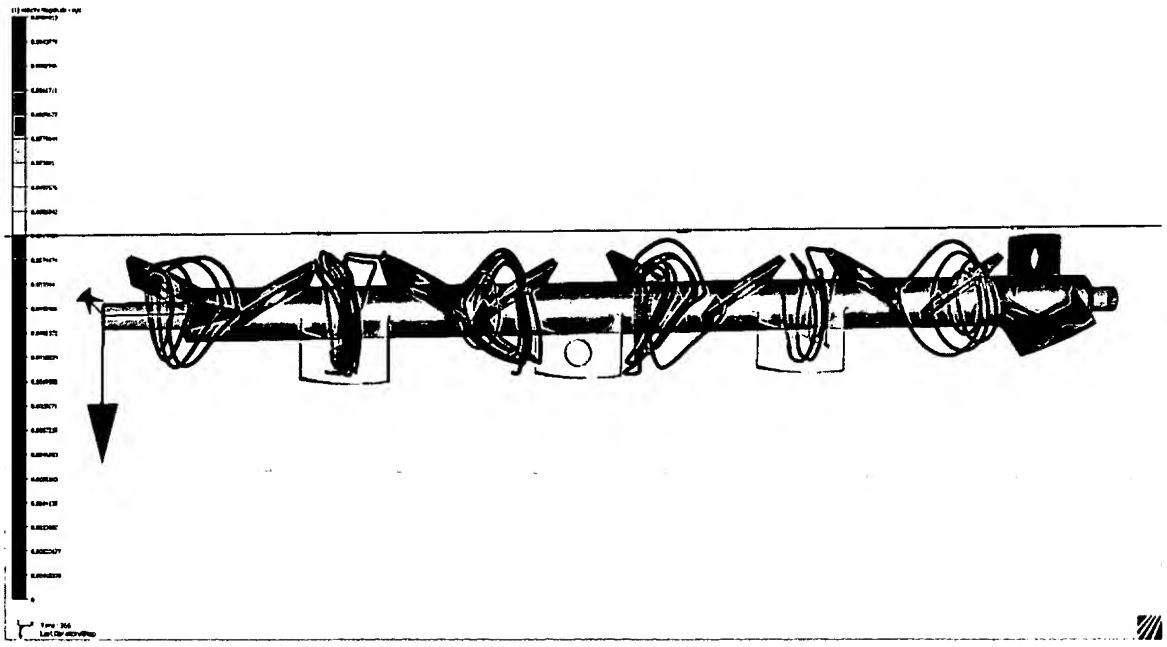

Figure I: Particle traces, with paddles removed for clarity

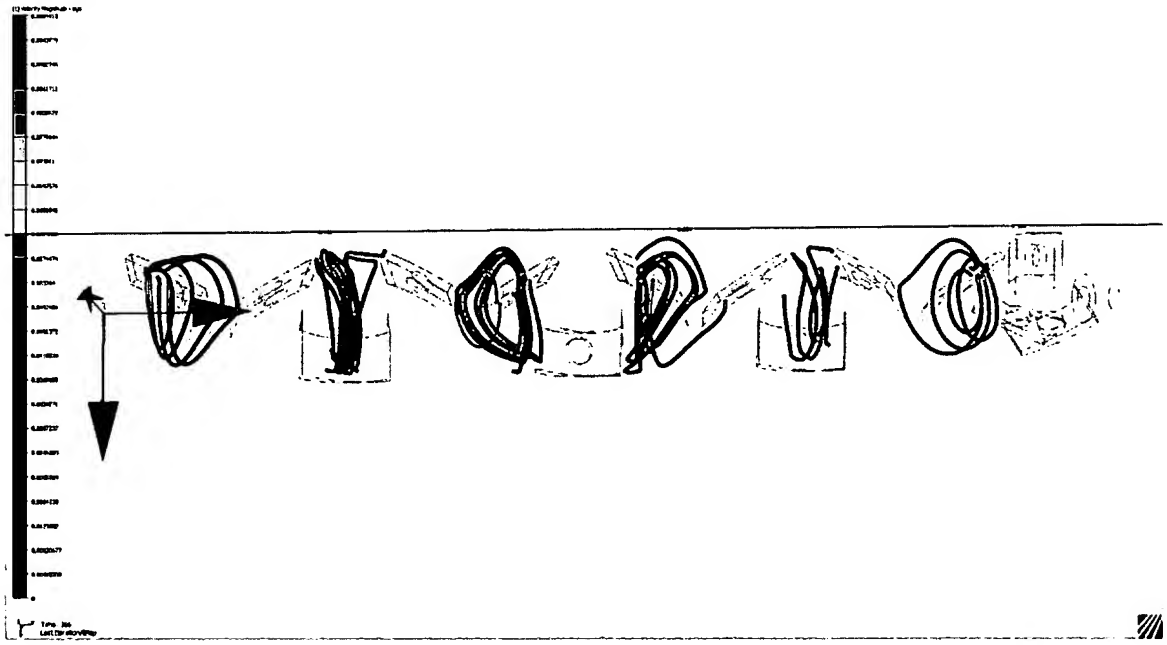

Figure H shows the movement paths of four particles clustered around each of the six blades highlighted with vectors in Figure E. Figure I shows the same view with no mechanical parts to obstruct the particle paths. The particles travel in circular orbits while following or being pushed by a paddle with some particles being bumped from one paddle to another (3 out of 24 in this sample).

Figure J: Particle traces, showing patterns and clumping, but limited lateral movement

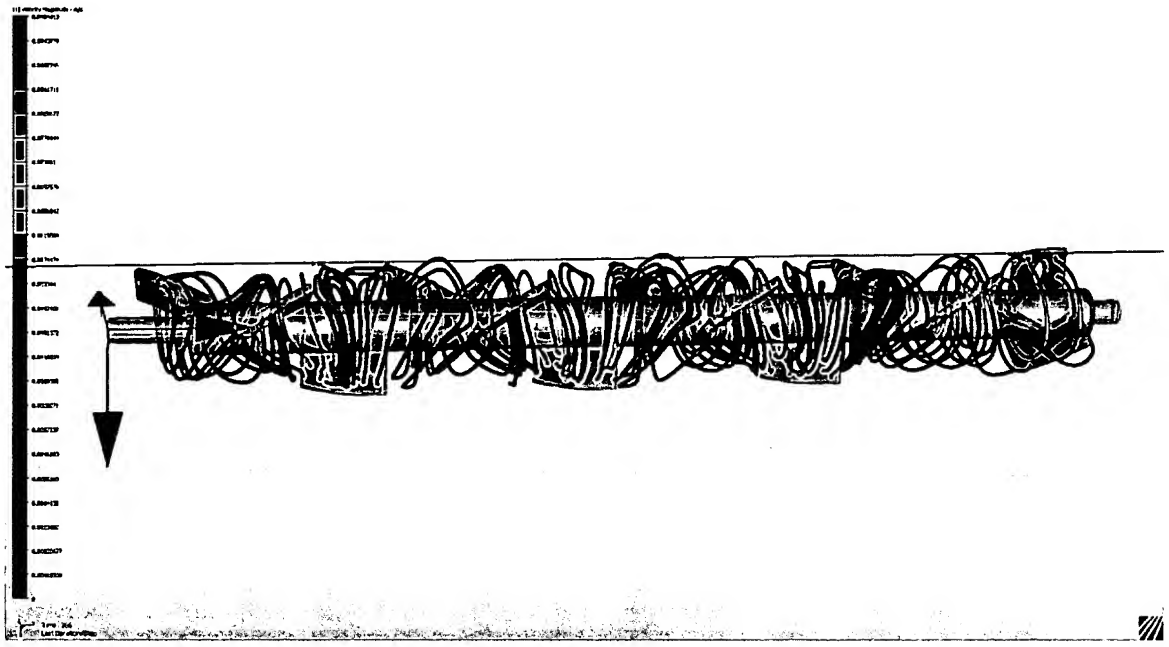

Figure K: Particle traces, with paddles removed for clarity

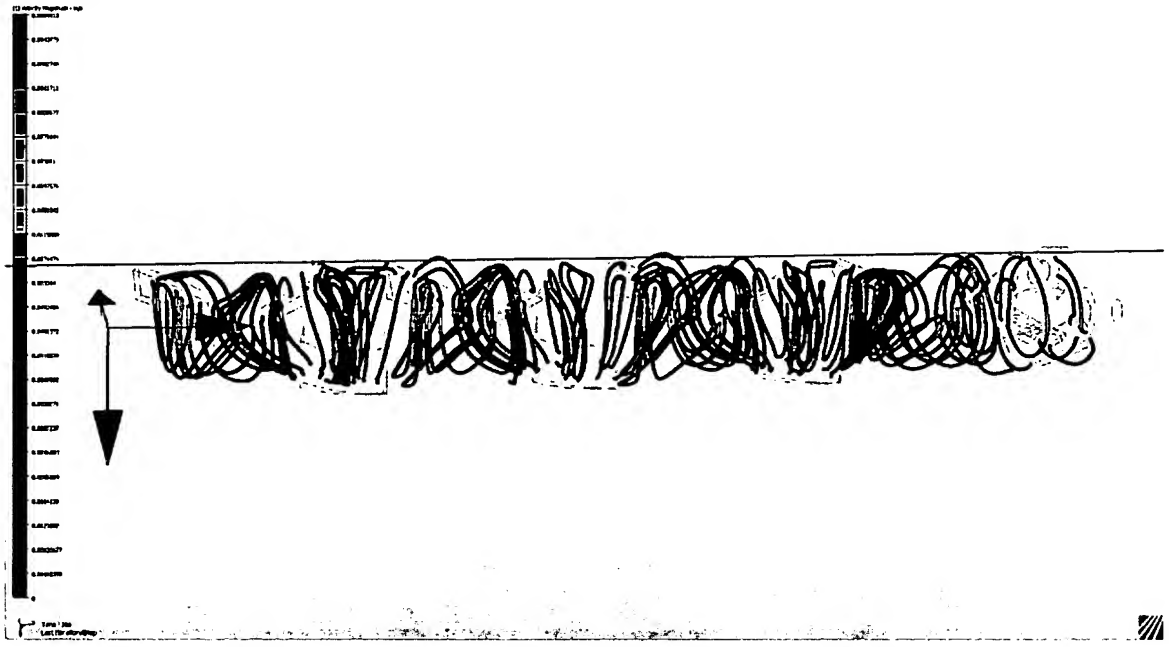

Figure J and Figure K show the above particles, plus additional traces for a total of over 100 randomly selected traces. Individual particles (or units of ice cream) tend to stay in the same axial position while orbiting in irregular shapes, almost like pasta spun around a fork. While occasional particles may interweave between others to create blending, the impeller motion and blending occurs in a spiral around the axis.

Study Conclusions:

Figure J and Figure K show over 100 randomly selected particles in the model, and not one of those particles traverses a circuit from the distal end to the proximal end, let alone circulates by returning to its origin. Instead each particle revolves around the X axis with some variation occurring depending upon where they strike the paddles.

Because every paddle is identical (with the exception of the scraper at the back), and equally spaced, any lateral motion that they may convey is counteracted equally by the paddles in front or behind them. This can be seen most clearly in Figure I, but the cumulative effects are most capably illustrated in the global pattern shown in Figure J and Figure K. No continuous circulation path from one end of the freeze tube assembly to the other end of the freeze tube assembly is discernable in the CFD analysis. There exists no loop, closed or otherwise.

Conclusions:

Ultimately, an examination of whether circulation appears in the Curry patent's freeze tube assembly 32 simply reinforces the importance of a "closed loop" circulation system in the sense that this application provides. In this application, the chamber, the circulation path, and the pump are all elements in a closed loop (of pipe) bounded by solid walls. The mechanical and physical closure of the looped system in this application means that the blending chamber has a defined entry and exit, and the pump ensures that recirculation happens according to its rate of flow rather than the speed of blending. In the Curry patent, the pump 30 is not part of a closed loop, since it simply pushes out material to be dispensed. Consequently, any circulation could only take place in the freeze tube assembly 32, but analysis here proves that it does not.

Indeed, this distinction is as much definitional as mechanical. Mixing could be defined as the intermingling of different materials until made homogenous, while circulation implies moving fluid around in an orderly manner. Mixing and circulating are antitheses: one destroys order while the other maintains it. Both cannot be expected to occur simultaneously in a closed chamber without discrete boundaries.

Instead, what is required is a two stage system: one chamber for mixing and another channel for circulation. The structure disclosed and claimed in this application achieves this with a motor dedicated to emulsifying and a separate motor dedicated to circulating/pumping. As such, the user can independently control two facets of the process. Mixing ensures that gas and fluids are initially homogenized and emulsified, while circulation maintains consistency by controlling which discrete portions are mixed and when. In ice cream, this distinction is important to avoid overmixing, which can cause the fat and the liquid components to separate in the ice cream mix. In this

application, this could be prevented by using an initial mixing cycle to emulsify, followed by rapid circulation combined with low RPM mixing, to ensure that the consistency remains uniform while limiting crystal formation and avoiding separation.

Furthermore, the combination of a circulation pump with a blender allows for desirable mixing characteristics, like the ability to produce ice cream in bands of flavor with variable mixing at the boundary. Such innovations are simply not possible with a one motor, one chamber system, such as the one shown in the Curry patent.

Curry's patent does not provide for a physically closed loop, does not provide for pump driven circulation, does not produce circulation within the emulsification chamber, and fails to produce ice cream in practice, since it has no break bar and nothing to arrest the ice cream from simply revolving as a single cylindrical frozen mass. As such, the Curry patent neither functions as described nor does it anticipate the novel aspects of a closed loop circulation system as described and claimed in this application.

References:

Byars, J. "Effect of a Starch-Lipid Fat Replacer on the Rheology of Soft-Serve Ice Cream," Journal of Food Science (Volume 67, Number 6, 2002). A copy is attached.

I hereby declare that all statements made herein of my own knowledge are true and that all statements made on information and belief are believed to be true; and further that these statements were made with the knowledge that willful false statements and the like so made are punishable by fine or imprisonment, or both, under 18 U.S.C. 1001 and that such willful false statements may jeopardize the validity of the application or any patent issued thereon.

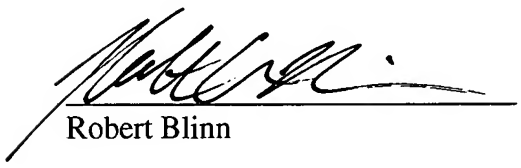

Robert Blinn

15 JUNE 2009

Date

Effect of a Starch-Lipid Fat Replacer on the Rheology of Soft-Serve Ice Cream

J. BYARS

ABSTRACT: The rheology of soft-serve ice creams prepared with Fantesk™, a starch-lipid composite, was compared to a commercial product. Fantesk™ describes a class of stable starch-lipid composites formed by steam-jet cooking, and is used in this case as a fat replacer. Waxy maize starch and butter were used, and the butter content was selected to give 0.5 to 1.1 wt% butter in the ice cream mix. Despite the lower level of fat, the overrun and rheological properties of the Fantesk™-based ice creams were similar to the commercial product when differences in the freezing behavior of the different formulations were accounted for.

Keywords: ice cream, rheology, soft-serve, Fantesk™

Introduction

ICE CREAM IS A COMPLEX FOOD FOAM SYSTEM CONSISTING OF air, fat, ice, and serum phases. Each of these phases affects the overall texture and quality of the final product. Rheology has proven to be useful for measuring the physical properties of ice cream, and for determining the effects of changes in composition. Sherman (1965, 1966) and Shama and Sherman (1966) modeled the creep behavior of ice cream and ice cream mix, and related changes in rheology to composition, temperature, and overrun. These researchers used a 6-element spring-and-dashpot model to determine the effect of each component on the overall structure. Dea and others (1984) measured the linear viscoelasticity of ice cream as a function of temperature. The temperature dependence of the storage modulus was used to relate its value to the volume fraction of ice. Goff and others (1995) investigated the effects of temperature, polysaccharide stabilizers, and overrun on the linear viscoelasticity of ice cream and ice cream mix. Their results showed that air bubbles and polysaccharide stabilizers also affected the storage modulus. Addition of polysaccharide increased the mix viscosity, while decreasing the storage and loss moduli and tan d. The influence of protein- and carbohydrate-based fat replacers on the linear viscoelasticity of ice cream was studied recently by Adapa and others (2000). They found that the fat replacers increased the viscous properties, but had little effect on the elastic properties. Much less attention has been given to the rheology of soft-serve ice cream. Goyal and others (1973) showed that the viscosity of soft-serve mixes increased slightly when glycerol monostearate, corn syrup, or dextrose was added, but no reports of the rheology of frozen soft-serve ice cream are available.

This work considers the rheology of both a commercial low-fat soft-serve ice cream and a series of soft-serve ice creams prepared with Fantesk™ (USDA). Fantesk™ is a stable starch-lipid composite prepared by co-jet cooking starch, lipid, and water with excess steam (Fanta and Eskins 1995; U.S. Patent 5,882,713). The result is a stable dispersion of 1 to 10-μm oil droplets encapsulated in a starch matrix. Composites can be prepared with up to 50% lipid by weight.The cooked product can be drum-dried and easily redispersed in water. Fantesk™ has previously been used to prepare reduced-fat cookies, cheese, and meat products (Brandt 2000).

The objective of this work was to compare the properties of a commercial soft-serve ice cream with those of reduced-fat soft-serve ice creams prepared with Fantesk™. The effects of Fantesk™ composition and concentration on the mix, the ice cream freezing and melting behavior, and the mix and ice cream rheology were studied.

Materials and Methods

Fantesk™ preparation

The Fantesk™ composite was prepared according to the procedure discussed by Fanta and Eskins (1995). Waxy maize starch (Staley, Decatur, Ill., U.S.A.) was suspended in distilled water at 15% dry weight basis with a Waring® (East Windsor, N.J., U.S.A.) blender. This slurry was passed through a jet cooker at 17 ml/s and combined with excess steam. The steam inlet pressure was 640 kPa, and the backpressure was 380 kPa. The cooked product was collected, blended with melted butter (Grade AA unsalted butter, 80% butterfat, Prairie Farms, Carlinville, Ill., U.S.A.), and then cooked again under the same conditions. The cooked starch was much more viscous than water, so blending the butter into previously cooked starch kept the butter dispersed until it passed through the jet cooker, thus assuring a more uniform final product. After the second cook, each product was drum-dried at 520 kPa steam pressure. The dried product was then milled (Fritsch Laboratory Cutting Mill, Idar-Oberstein, Germany) to pass through a 4-mm mesh.

Ice cream mix

Fantesk™-based soft-serve mixes were prepared with different levels of Fantesk™, and with Fantesk™ having different butter:starch ratios. The compositions of each mix and its fat content are shown in Table 1. The composition of the mixes was selected to yield an acceptable frozen product without any obvious sensory defects, rather than to duplicate the rheology of the commercial product. The level and composition of Fantesk™ was varied within the range that gave acceptable products. The mixes denoted as 3%, 4%, and 5% Fantesk™ used an identical butter:starch ratio of 2:5,

Table 1—Composition of ice cream mixes with ingredient amounts in weight percent

	3% Fantesk™	4% Fantesk™	5% Fantesk™	3.4% Fantesk™	Commercial
butter:starch	2:5	2:5	2:5	1:5	
skim milk	75.9	75.1	74.3	75.6	
NFDM	3.9	3.9	3.9	3.9	
corn syrup	11.1	11.0	10.9	11.1	
Sucrose	6.1	6.0	6.0	6.0	
% fat in mix	0.7	0.9	1.1	0.5	3.5
wt% solids	30.3	30.0	31.2	29.9	31.1
density [kg/m^3]	1116	1120	1122	1118	1101

Table 2—Properties of frozen soft-serve ice cream

	% overrun	$T_{transition}$ [°C]	$T_{measurement}$ [°C]	$T_{melting}$ [°C]	melt rate [g/100g/min]
3% Fantesk™	48.9 ± 3.1	-6.4 ± 0.3	-4.7	-4.0 ± 0.7	2.55
4% Fantesk™	49.4 ± 2.5	-5.7 ± 0.3	-4.0	-3.0 ± 0.7	2.44
5% Fantesk™	46.9 ± 1.6	-5.7 ± 0.3	-4.0	-3.0 ± 0.7	2.67
3.4% Fantesk™	49.8 ± 3.0	-5.7 ± 0.3	-4.0	-3.0 ± 0.7	2.50
Commercial	51.5 ± 3.5	-7.3 ± 0.3	-5.6	-4.7 ± 0.7	2.34

whereas the Fantesk™ in the mix denoted "3.4% Fantesk™" used about half as much butter. The amount of starch present in the mix was the same for the 3.4% and 4% Fantesk™ mixes. In each case, the milled Fantesk™ was added to the skim milk while heating and stirring, which readily dispersed the Fantesk™. The non-fat dry milk solids (Carnation instant nonfat dry milk, Nestlé USA, Solon, Ohio, U.S.A.), corn syrup (Karo light corn syrup, Best Foods, Englewood Cliffs, N.J., U.S.A.), and sucrose were then added as the temperature was brought to 80 °C, where it was held for 15 min. The mix was then transferred to a plastic bag and quenched in an ice bath. The cooled mix was then stored at 4 °C overnight. The commercial soft-serve mix (Prairie Farms, Carlinville, Ill., U.S.A.) contained 3.5% fat and was used as received. The density of each mix was measured in a calibrated pycnometer at 25 °C, and the total-solids concentration was measured by freeze-drying.

Ice cream preparation

Ice creams were prepared in an Electro-Freeze® CS2 soft-serve gravity-fed freezer (East Moline, Ill., U.S.A.). As discussed below, the draw temperature for each soft-serve was based on its freezing properties. The draw temperature could not be controlled precisely, but was always within 0.5 °C of the measurement temperature for each soft-serve. To prevent melting before the rheological measurements could be conducted, samples were collected in a Dewar flask. The mix feed assembly, which controls the amount of air incorporated into the final product, was maintained in the same position for all tests. The overrun for each sample is given in Table 2. Measurements of the overrun at a given time were reproducible within 1% overrun, so the standard deviation given in Table 2 indicates a variation in overrun during a set of experiments. The differences in overrun between samples were not statistically significant. No differences in the rheological properties of the soft-serve ice creams were observed for changes of the overrun in this range. Table 2 indicates that, despite the lower fat level in the Fantesk™ and the fact that the fat was in a starch composite, an overrun of nearly 50% was still obtained.

Rheological measurements

The viscosities of the ice cream mixes were measured on a Rheometrics® ARES controlled-strain fluids rheometer (Rheometric Scientific, Piscataway, N.J., U.S.A.), using a 50-mm diameter, 0.04 radian cone. A circulating water bath was used to maintain the temperature of the bottom plate at 6.0 ± 0.1 °C. Measurements on the prepared ice cream were conducted on a Rheometrics® ARES controlled-strain melts rheometer with 25-mm dia serrated parallel plates. The rheometer was equipped with an air convection oven and a mechanical chiller to allow temperature control within ± 0.1 °C. The measurement temperature for each ice cream is given in Table 2, and the method for determining this temperature is discussed below. Reported results are mean values of at least 2 measurements, and a fresh sample was used for each measurement. Repeated measurements were typically within 10% of each other, but some varied by as much as 20%. Stress relaxation experiments at large strain were especially difficult to reproduce exactly. Data were analyzed by analysis of variance, and significance of differences was defined at $p \leq 0.05$. Fits of the linear viscoelastic spectra were obtained using a Levenberg-Marquardt algorithm with MathCad™ software (MathSoft, Cambridge, Mass., U.S.A.). Integrations of the K-BKZ equation were also performed with MathCad. The intrinsic viscosity of the jet-cooked starch was measured using a Schott AVS 360 automated viscosity system (Hofheim, Germany).

Results and Discussion

RHEOLOGICAL RESULTS ARE PRESENTED FOR 5 DIFFERENT soft-serve ice creams: a commercial product and 4 different Fantesk™-based mixes. The Fantesk™ concentration and composition were selected in the range that gave acceptable products. Three different starch levels and 4 different fat levels were studied.

The viscosities of the mixes at 6 °C are shown in Figure 1 for each mix. No slip was observed for any of the mixes. Upon startup of a steady shear flow, the viscosity of each mix increased to a steady value, with an overshoot at higher rates. The viscosity of the 3% Fantesk™ mix approaches a constant value at low shear rates, but each of the other mixes is shear-thinning across the entire range of shear rates mea-

Table 4—Zero-shear-rate viscosity and Maxwell relaxation time from linear viscoelastic spectrum, and the predictions of the K-BKZ model for the viscosity and relaxation time at a shear rate of 1 s^{-1}

	η_0 [10^5 Pa·s]	λ_0 [s]	$\eta(\dot{\gamma} = 1\ s^{-1})$ [Pa·s]	$\lambda(\dot{\gamma} = 1\ s^{-1})$ [s]
3% Fantesk™	7.8	77	1220	0.019
4% Fantesk™	7.6	75	2110	0.018
5% Fantesk™	7.7	77	1600	0.018
3.4% Fantesk™	7.7	80	1440	0.017
Commercial	5.6	88	1350	0.022

Table 3—Damping function coefficients from stress relaxation experiments

	K	a_1	a_2
3% Fantesk™	0.93	0.61	0.056
4% Fantesk™	0.97	0.42	0.040
5% Fantesk™	0.97	0.39	0.034
3.4% Fantesk™	0.96	0.49	0.046
Commercial	0.92	0.64	0.049

sured, and no zero-shear-rate viscosity could be obtained for the sensitivity of this rheometer. The 5% Fantesk™ mix had the highest viscosity, and its viscosity was on average 1.8 times higher than for the 3.4% mix. The 3.4% and 4% mixes had the same total starch content, but they had slightly different viscosities at low shear rates. This is most likely due to batch-to-batch variations in the degradation of the starch in the jet cooker. The Fantesk™ used for the 3%, 4%, and 5% mixes all came from the same batch. The viscosity of the commercial mix decreases more sharply with shear rate than the Fantesk™-based mixes, so although its viscosity is about 1.4 times higher than the viscosity of the 3.4% Fantesk™ mix at the lowest rates, it is only 0.6 times as high at high shear rates. The increase in viscosity with starch content is not surprising, considering the high molecular weight of the starch in the Fantesk™. Even after passing through the jet cooker twice, waxy maize starch has an intrinsic viscosity of 115 ml/g in 90/10 dimethyl sulfoxide/water, which corresponds to a molecular weight of 8×10^7 g/mol (Millard and others 1997). However, amylopectin is highly branched and water is a poor solvent for amylopectin, so the effect of the addition of high molecular weight amylopectin on the solution viscosity is not as great as for fully expanded random coil molecules. The changes in viscosity of the Fantesk™-based mixes had no observable effect on the operation of the soft-serve machine.

Changes in the mix composition will also affect the freezing behavior of the final product, and these changes must be taken into account in order to compare samples under similar conditions. Ideally, the ice phase fraction would be held constant, but this could not be measured directly. Measurements of the freezing point depression for each mix would give an indication of different freezing behavior, but would not relate directly to the ice fraction of the ice cream below its freezing point. A more complete understanding of the temperature dependence of the soft-serve ice creams can be obtained by measuring the complex viscosity, η^*, as a function of temperature, as shown in Figure 2. A sample was placed in the rheometer and equilibrated to an initial temperature between −10 °C and −12 °C. The complex viscosity at a frequency of 1 rad/s was measured, and then the tem-

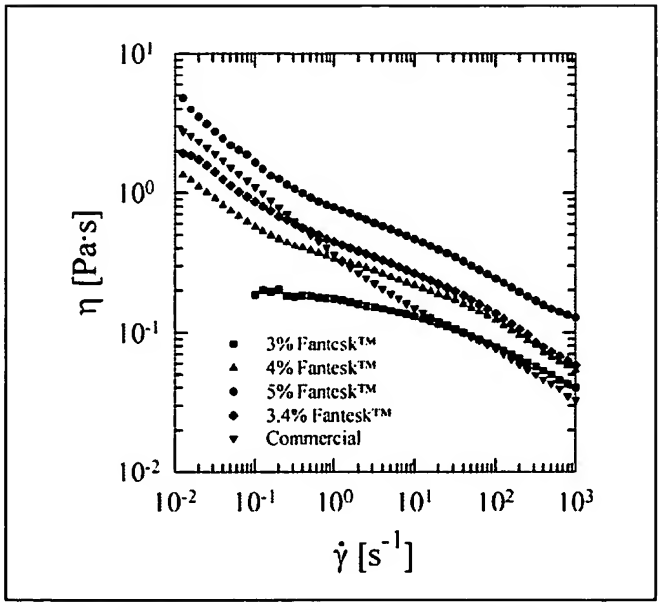

Figure 1—Viscosity of soft-serve mixes at 6 °C

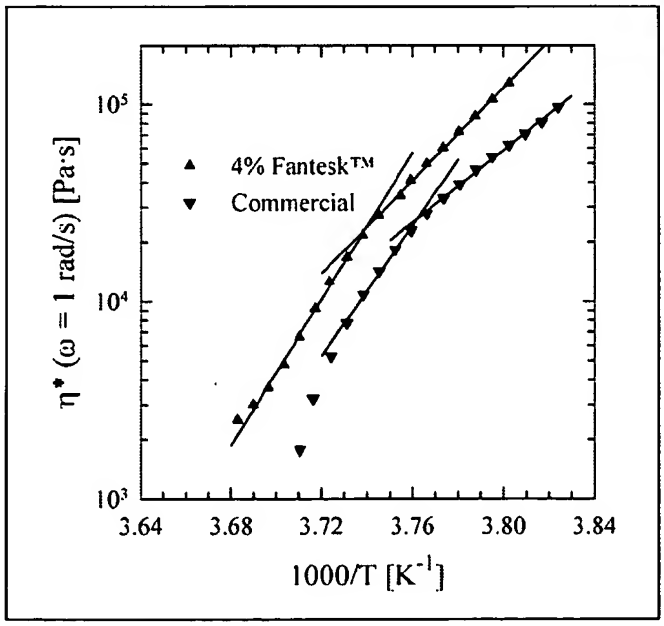

Figure 2—Temperature dependence of the complex viscosity at a frequency of 1 rad/s of the 4% Fantesk™ and commercial soft-serve ice creams. Lines are fits to the data showing the 2 regions of Arrhenius temperature dependence.

perature was increased in 0.5 °C steps. The sample was allowed to equilibrate for 2 min at each temperature before measuring the complex viscosity, which was long enough to reach a constant value. Three distinct regions of behavior are seen on the Arrhenius plot in Figure 2. At low temperatures there is a region of constant slope, followed by a sharp transition to a region of higher slope, indicating a change in the flow mechanism at the transition temperature. Goff and others (1993, 1995) have discussed the importance of the serum phase's freeze concentration in determining the structure of ice cream. They attributed a change in the temperature dependence of the dynamic properties to close packing of ice crystals at a critical temperature, and much lower modulus values were measured above this temperature. Although the ice phase fraction will change throughout the temperature range in Figure 2, the change in slope implies a qualitative change in the mobility of the serum phase such that, at higher temperatures, further melting of ice leads to much greater changes in the complex viscosity than at lower temperatures. Because the exact nature of this change is not known, the intersection of the fits to the data in the 2 temperature regimes is simply called a transition temperature in Table 2. At the highest temperatures, the sample has melted and there is no clear trend. The final melting point is not defined as clearly as the lower transition temperature. The values given in Table 2 are based on the final point that lay on the melting curve, which will necessarily underestimate the true melting point by up to 0.4 °C. The difference between the transition temperature and the melting temperature was nearly constant for all samples at 2.4 to 2.7 °C. Assuming that the ice phase fraction changed from zero at the melting temperature to the same value at the transition temperature, temperatures at the same relative position in this range should have the same ice phase fraction even as the temperature range shifts, depending on the freezing properties of the mix. Since the transition temperature could be determined more precisely, all measurements for each sample were conducted 1.7 °C above the transition temperature, and the draw temperature was adjusted to be as close to the measurement temperature as possible. The activation energy for the Fantesk™ samples at $T_{transition} > T > T_{melting}$ was 430 ± 90 kJ/mol, whereas for the commercial soft-serve it was 340 ± 60 kJ/mol. This corresponds to a change of up to 100% in the complex viscosity for a 1 °C change in temperature, indicating that the ice fraction has a dramatic effect on the properties of the ice cream. The ratio tan δ G"/G' increased about 10% as the temperature was decreased below $T_{transition}$, and then dropped sharply as the sample melted.

The linear viscoelastic response of the products can be obtained by measuring the storage modulus G' and the loss modulus G" in small amplitude oscillatory shear flow over a range of frequencies. Figure 3a and 3b show G' and G" for all of the soft-serves studied. The range of strains for which a linear viscoelastic response was observed depended strongly on frequency. The strain used for the measurements in Figure 3 varied from 0.01% at high frequency to 0.3% at low frequency. The results show that there was little effect of variations in the Fantesk™ formulations, and that the Fantesk™ samples had greater elasticity than the commercial product. The 3.4% and 4% Fantesk™ samples were nearly identical at all frequencies. These samples contained the same amount of starch, but the 3.4% Fantesk™ sample had about half as much fat. At low frequency, G' for these samples was more than twice as high as G' for the commercial sample, while at the highest frequencies the difference was only about 30%. Likewise, G" was about 70% higher for the Fantesk™ samples at low frequencies, but all of the samples were within 10% of each other at high frequencies. Dynamic property measurements at low frequencies measure the effects of longer relaxation times in the sample. Although the contribution of each phase to the overall viscoelastic response is unknown, the fact that the overrun is similar for each sample, and that the temperature dependence implies that each sample has the same ice phase fraction, the differences in Figure 3 may be due to the contribution of the serum phase. As the serum phase is freeze-concentrated, the relaxation time of the high

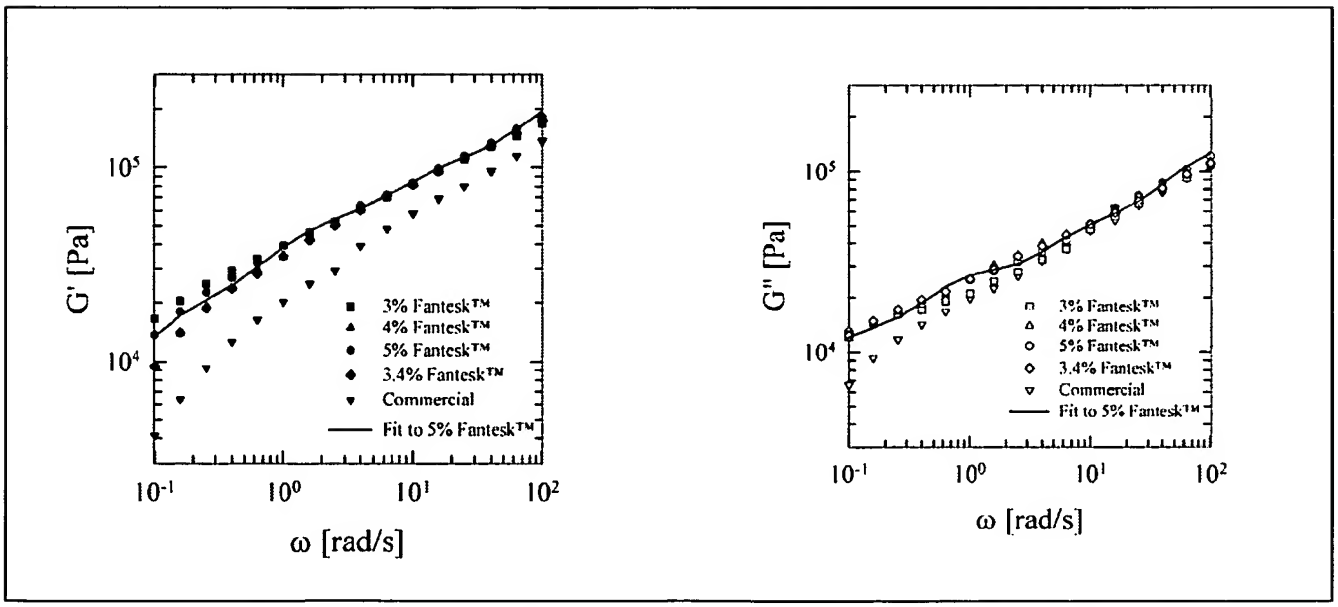

Figure 3—The storage and loss moduli for the soft-serve ice creams. The curves are the predictions of a 6-mode Maxwell model of the properties of the 5% Fantesk sample.

molecular-weight starch will become more important. This could explain why the 5% Fantesk™ has a higher storage modulus than the 3.4% and 4% Fantesk™ samples at low frequency. However, G' for the 3% Fantesk™ sample is higher still. If the starch in the serum phase accounts for differences in G' at low frequency, the lower measurement temperature for the 3% Fantesk™ sample would be expected to have a longer relaxation time and therefore a higher storage modulus, although this effect cannot be quantified. A more important point in Figure 3 illustrates that the properties of the 3% Fantesk™ are within 10% of the other samples at most frequencies, despite the 0.7 °C difference in measurement temperature. Based on the activation energies given above, a temperature change of 0.7 °C should lead to a difference of 65%. The fact that all of the Fantesk™ samples agree so closely justifies the method of determining the measurement temperature in Figure 2, and further shows that the ice phase fraction is the major influence on the rheology of soft-serve ice cream.

Although measurements of the linear viscoelastic properties of ice cream have proven useful, the processing and consumption of ice cream involve strains well outside the linear region. A complete rheological characterization of ice cream therefore also requires measurements of its response to nonlinear deformations. A typical measurement at high strains is the viscosity, but the viscosities of the frozen products could not be measured due to slip of the sample in the rheometer. Instead, a series of stress relaxation experiments was performed over a range of strains that extended beyond the linear region. A strain between 0.5% and 100% was instantaneously applied to the sample, and the stress relaxation modulus, G, was measured as a function of time. The results for the 5% Fantesk™ ice cream are shown in Figure 4. As the strain is increased, the stress relaxation modulus decreases, although its time dependence remains the same at all strains. The downward shift of the stress relaxation modulus with increasing strain can be used to define a damping function, $h(\gamma)$. The damping function is defined as the ratio of the stress relaxation modulus at a given strain to the value at strains in the linear region. The damping function for these materials can be described by a double exponential function:

$$h(\gamma) = K\exp(-a_1\gamma) + (1-K)\exp(-a_2\gamma) \quad (1)$$

The values of K, a_1, and a_2 for each sample are given in Table 3. The shape of the damping function is similar for all samples for strains up to 10%, but as indicated by the lower value of K (that is, higher 1-K), $h(\gamma)$ is larger for the 3% Fantesk and commercial ice creams at intermediate strains. Because h(g) is normalized to the low-strain values for each sample, the values in Table 3 only indicate the qualitative differences between samples, not absolute differences in the stress relaxation modulus at a given strain.

The samples can be further characterized by a linear viscoelastic spectrum $\{G_i, \lambda_i\}$, which can be obtained for each sample by fitting a multimode Maxwell model to the results of the frequency sweeps:

$$G'(\omega) = \sum_i \frac{G_i\lambda_i^2\omega^2}{1+(\lambda_i\omega)^2} \quad (2)$$

$$G''(\omega) = \sum_i \frac{G_i\lambda_i\omega}{1+(\lambda_i\omega)^2} \quad (3)$$

or the stress relaxation modulus at low strains:

$$G(t) = \sum_i G_i \exp(-t/\lambda_i) \quad (4)$$

The same set of $\{G_i, \lambda_i\}$ should fit the results of each experiment, so a fit was obtained to minimize the total error, with equal weight given to the frequency sweep and stress relaxation experiments. This combined fit extends the range of time constants that can be determined, since the frequency

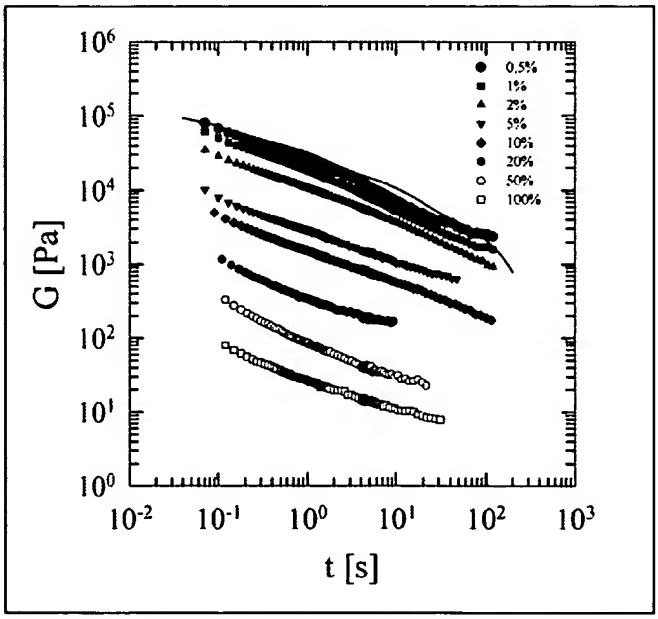

Figure 4—The stress relaxation modulus at various strain levels for the 5% Fantesk™ soft-serve ice cream

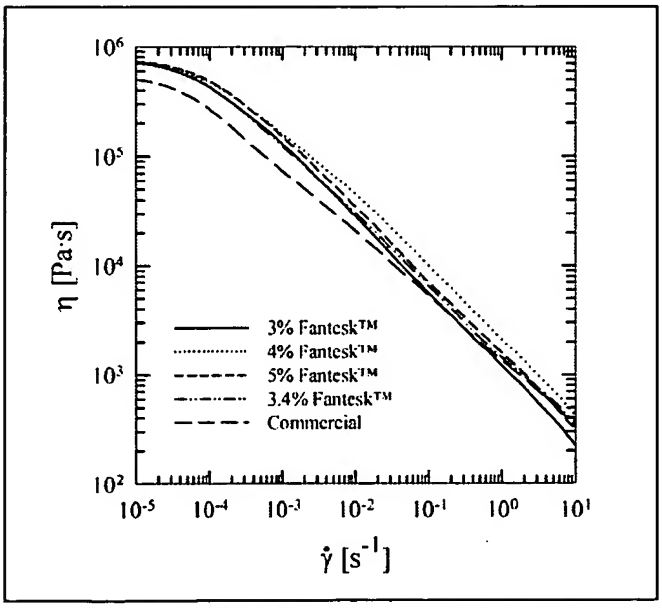

Figure 5—The predictions of the K-BKZ constitutive equation for the viscosity of the soft-serve ice creams

sweep will be characterized by time constants that are the inverse of the frequency range studied (λ = 0.01 – 10 s), whereas the stress relaxation will be characterized by time constants that depend on the length of the experiment (λ = 0.1 – 100 s). Six relaxation modes were used for each product. The individual values $\{G_i, \lambda_i\}$ in this case are essentially fitting parameters, and no physical meaning can be assigned to them, other than noting that soft-serve ice cream must be characterized by a broad range of relaxation times. However, the linear viscoelastic spectra can be used to compare different materials by calculating a zero-shear-rate viscosity $\eta_0 = \sum G_i\lambda_i$ and a Maxwell relaxation time $\lambda_0 = \sum G_i\lambda_i^2 / \sum G_i\lambda_i$ These results are summarized in Table 4. As expected from Figure 3, the values for all of the Fantesk™ products are similar, and the commercial product has a lower viscosity. The longer relaxation time for the commercial product is a result of a slower decay of its stress relaxation modulus. The fit for the 5% Fantesk™ is shown in Figure 3 and 4. Note that extrapolating the predictions of Eq. 3 beyond 100 s predicts a sharp decline, whereas the data do not indicate any change in behavior. The maximum measurement time in Figure 4 is limited by the sensitivity of the rheometer, and if the data continued the same trend at longer times, higher values of h_0 and l_0 would be predicted. The values in Table 3 must therefore be viewed as lower bounds on h_0 and λ_0, rather than true zero-shear-rate values.

Even though the true η_0 and λ_0 values are higher, the values in Table 4 are still much higher than would be expected based on the consumption of soft-serve ice cream. The sensitivity of the ice cream's structure to deformation can be seen in Figure 4, where the stress relaxation modulus drops sharply with increasing strain. Based on the linear viscoelastic spectrum and the damping function obtained above, it is possible to estimate the viscosity and relaxation time at more typical shear rates by using the K-BKZ constitutive equation:

$$\tau(t) = \int_{-\infty}^{t} m(t-t')h(\gamma)\mathbf{B}(t,t')dt' \quad (5)$$

where $\tau(t)$ is the stress tensor, m(t-t') is the memory function,

$$m(t-t') = \sum_i \frac{G_i}{\lambda_i}\exp[-(t-t \quad (6)$$

h(g) is the damping function, and B(t, t') is the Finger strain tensor, which describes the deformation applied to the sample. The K-BKZ model is an empirical model that does not explicitly account for the complex structure of the ice cream, although the memory function and damping function will obviously depend on the fluid being studied. The model only assumes that the effects of time and strain are separable: this assumption is justified by the fact that the curves for the stress relaxation modulus in Figure 4 remain nearly parallel for all strains. Equation 5 can then be used to predict the viscosity as a function of shear rate, as shown in Figure 5. Because the predictions of the K-BKZ model could not be validated for soft-serve ice cream in other nonlinear flows, the quantitative accuracy of the results of Figure 6 cannot be determined. However, an important feature of the results is that, despite the different formulations, all products have similar shear-rate dependence at high shear rates, and the viscosity is predicted to drop by over 2 orders of magnitude at a shear rate of 1 s^{-1}. A shear rate-dependent relaxation time can also be defined as

$$\lambda(\dot{\gamma}) = \frac{\Psi_1(\dot{\gamma})}{2\eta(\dot{\gamma})} \quad (7)$$

where $\Psi_1(\dot{\gamma})$ is the first normal stress coefficient. As shown in Table 4, the relaxation time at 1 s^{-1} is over 3 orders of magnitude smaller than predicted by linear viscoelastic measurements. For the form of the damping function used in Eq. 1, the K-BKZ model predicts aphysically large decreases in the viscosity at high shear rates (Larson and Monroe 1984), so the viscosity cannot be predicted at shear rates higher than 10 s^{-1} in this case.

Conclusions

A COMPLETE RHEOLOGICAL CHARACTERIZATION WAS OBTAINED for a commercial soft-serve ice cream, and for 4 different ice creams made with a starch-lipid fat replacer. When differences in the freezing behavior were taken into account, only minor changes were observed between Fantesk™-based ice creams with different fat and starch levels. All of the Fantesk™-based ice creams were more elastic than the commercial product in small amplitude oscillatory shear flow. Stress relaxation experiments combined with the results of linear viscoelasticity measurements allowed the viscosity in shear flow to be calculated. These predictions showed that the viscosities of all formulations are expected to have similar shear-rate dependence. Measurements of mix properties, overrun, and melting behavior also showed that the Fantesk™-based ice creams were similar to the commercial product.

References

Adapa S, Dingeldein H, Schmidt KA, Herald TJ. 2000. Rheological properties of ice cream mixes and frozen ice creams containing fat and fat replacers. J Dairy Sci 83:2224-2229.

Brandt LA. 2000. Novel ingredients for lowfat foods. Prep Foods (Oct 2000):49-52.

Dea ICM, Richardson RK, Ross-Murphy SB. 1984. Characterization of rheological changes during the processing of food materials. In: Phillips GO, Wedlock DJ, Williams PA, editors. Gums and stabilizers for the food industry. Vol. 2. Oxford: Pergamon Press. P 357-366.

Fanta GF, Eskins K. 1995. Stable starch-lipid compositions prepared by steam jet cooking. Carbohydr Polym 28:171-175.

Fanta GF, Eskins K, inventors; Agricultural Research Service, United States Department of Agriculture, assignee. March 16, 1999. Non-seperable compositions of starch and water-immiscible organic materials. U.S. patent 5,882,713.

Goff HD, Caldwell KB, Stanley DW, Maurice TJ. 1993. The influence of polysaccharides on the glass transition in frozen sucrose solutions and ice cream. J Dairy Sci 76:1268-1277.

Goff HD, Freslon B, Sahagian ME, Hauber TD, Stone AP, Stanley DW. 1995. Structural development in ice cream – dynamic rheological measurements. J Texture Stud 26:517-536.

Goyal GK, Srinivasan MR. 1973. The quality of soft-serve ice cream as influenced by the levels of fat, emulsifier, sucrose substitutes, and processing conditions. J Food Sci Technol 10:122-124.

Larson RG, Monroe K. 1984. The BKZ as an alternative to the Wagner model for fitting shear and elongational flow data of an LDPE melt. Rheol Acta 23:10-13.

Millard MM, Dintzis FR, Willett JL, Klavons JA. 1997. Light-scattering molecular weights and intrinsic viscosities of processed waxy maize starches in 90% dimethyl sulfoxide and H_2O. Cereal Chem 74(5):687-691.

Shama F, Sherman P. 1966. The texture of ice cream: 2. Rheological properties of frozen ice cream. J Food Sci 31:699-706.

Sherman P. 1965. The texture of ice cream. J Food Sci 30:201-211.

Sherman P. 1966. The texture of ice cream: 3. Rheological properties of mix and melted ice cream. J Food Sci 31:707-716.

MS 20010127 Submitted 3/11/01, Accepted 7/9/01, Received 7/17/01

The technical assistance of Steven A. Lyle and A.J. Thomas is gratefully acknowledged. This work was financially supported by the United States Department of Agriculture. Names are necessary to report factually on available data; however, the USDA neither guarantees nor warrants the standard of the product, and the use of the name by the USDA implies no approval of the product to the exclusion of others that may also be suitable.

Author Byars is affiliated with the National Center for Agricultural Utilization Research, 1815 N. University Street, Peoria, IL 61604. Direct inquiries to author at Byars (E-mail: byarsja@ncaur.usda.gov).